MOLECULAR AND CELLULAR BIOLOGY, July 2000, p. 5175–5183 Vol. 20, No. 14
0270-7306/00/$04.00+0

Hepatocyte Nuclear Factor 3β (Foxa2) Is Dispensable for Maintaining the Differentiated State of the Adult Hepatocyte

NEWMAN J. SUND,[1] SIEW-LAN ANG,[2]* SARA DUTTON SACKETT,[1] WEI SHEN,[1] NATHALIE DAIGLE,[2] MARK A. MAGNUSON,[3] AND KLAUS H. KAESTNER[1]*

Department of Genetics, University of Pennsylvania School of Medicine, Philadelphia, Pennsylvania 19104-6145[1]; Institut de Génétique et de Biologie Moléculaire et Cellulaire, CNRS/INSERM/Université Louis Pasteur, 67404 Illkirch Cedex, France[2]; and Department of Molecular Physiology and Biophysics, Vanderbilt University School of Medicine, Nashville, Tennessee 37232[3]

Received 21 December 1999/Returned for modification 3 February 2000/Accepted 5 April 2000

Liver-specific gene expression is controlled by a heterogeneous group of hepatocyte-enriched transcription factors. One of these, the winged helix transcription factor hepatocyte nuclear factor 3β (*HNF3*β or *Foxa2*) is essential for multiple stages of embryonic development. Recently, *HNF3*β has been shown to be an important regulator of other hepatocyte-enriched transcription factors as well as the expression of liver-specific structural genes. We have addressed the role of *HNF3*β in maintenance of the hepatocyte phenotype by inactivation of *HNF3*β in the liver. Remarkably, adult mice lacking *HNF3*β expression specifically in hepatocytes are viable, with histologically normal livers and normal liver function. Moreover, analysis of >8,000 mRNAs by array hybridization revealed that lack of *HNF3*β affects the expression of only very few genes. Based on earlier work it appears that *HNF3*β plays a critical role in early liver development; however, our studies demonstrate that *HNF3*β is not required for maintenance of the adult hepatocyte or for normal liver function. This is the first example of such functional dichotomy for a tissue specification transcription factor.

Hepatic gene expression is controlled by a diverse set of transcription factors, none of which is expressed exclusively in the liver. Among these are the hepatocyte nuclear factor 3 α, β, and γ proteins (HNF3α, HNF3β, and HNF3γ, respectively), which were first discovered by their ability to bind to the promoters of the liver-specific genes encoding α1-antitrypsin and transthyretin (8, 20, 21). The *HNF3* genes are closely related to the *Drosophila melanogaster* gene *forkhead*, which is essential for the proper formation of the foregut and hindgut (32). This fact together with the observation that the mouse *HNF3* genes are expressed early during the formation of definite endoderm led to the hypothesis that the HNF3 proteins function in mammalian liver and gut development (3, 23, 27).

Recently, the nomenclature of the winged helix/forkhead transcription factor gene family has been revised, and according to this new nomenclature the genetic loci encoding HNF3α, HNF3β, and HNF3γ are now known as *Foxa1*, *Foxa2*, and *Foxa3*, respectively, in mouse (*Fox* refers to *forkhead box*) (17).

Analysis of the crystal structure of the DNA binding domain of HNF3γ showed a striking similarity to the winged helix domain of linker histones (7). The HNF3 proteins can bind to and reposition nucleosomes in the albumin gene which correlates with an active albumin enhancer (6, 22, 29). As the HNF3 proteins can alter chromatin and are the earliest known factors expressed in the prehepatic endoderm, the HNF3 proteins were proposed to act as genetic potentiators of the hepatic differentiation program (34).

During formation of the definite endoderm, *HNF3*β is activated first, followed by *HNF3*α, and finally *HNF3*γ (3, 23, 27). *HNF3*β is required for the development of the node and for visceral endoderm formation because these structures are missing or abnormal in embryos homozygous for a targeted null mutation in the *HNF3*β gene (2, 10, 33). However, the functions of *HNF3*β in the differentiation of the hepatic primordium or in hepatic metabolism could not be addressed using the *HNF3*β null allele, as even embryos obtained from tetraploid embryonic stem (ES) cell aggregations lacked foregut and midgut endoderm (10).

In contrast to the *HNF3*$\beta^{-/-}$ mice, embryos deficient for *HNF3*α or *HNF3*γ develop normally to term and show no obvious morphological liver phenotype (15, 16, 28). *HNF3*α mutant mice had unchanged expression of liver-specific HNF3 target genes involved in metabolism and glucose homeostasis. However, the transcription of several HNF3 targets was reduced by 50 to 70% in the *HNF3*γ mutants. Due to the similarity of the HNF3 proteins it seems likely that these transcription factors can at least partially compensate for each other during liver development, when all three genes are expressed concurrently.

Recently, the regulatory function of *HNF3*β has been studied in visceral endoderm derived from *HNF3*$\beta^{-/-}$ embryoid bodies in vitro (12). In this model, the lack of *HNF3*β resulted in a reduction of the mRNA levels for the transcription factors *HNF1*α and *HNF4*α and a complete elimination of the *HNF3*α transcript, suggesting that *HNF3*β regulates a transcription factor network required for differentiation and metabolism (12). To test the role of *HNF3*β in regulating the hepatic transcriptional program in vivo, we have generated mice lacking *HNF3*β specifically in hepatocytes using the Cre-loxP recombination system. Here we describe the liver-specific gene

* Corresponding author. Mailing address for Klaus H. Kaestner: Department of Genetics, University of Pennsylvania School of Medicine, 415 Curie Blvd., Philadelphia, PA 19104-6145. Phone: (215) 898-8759. Fax: (215) 573-5892. E-mail: kaestner@mail.med.upenn.edu. Mailing address for Siew-Lan Ang: Institut de Génétique et de Biologie Moléculaire et Cellulaire, CNRS/INSERM/Université Louis Pasteur, B.P. 163, 67404 Illkirch Cedex, France. Phone: 333 88 653342. Fax: 333 88 653 201. E-mail: siew-lan@titus.u-strasbg.fr.

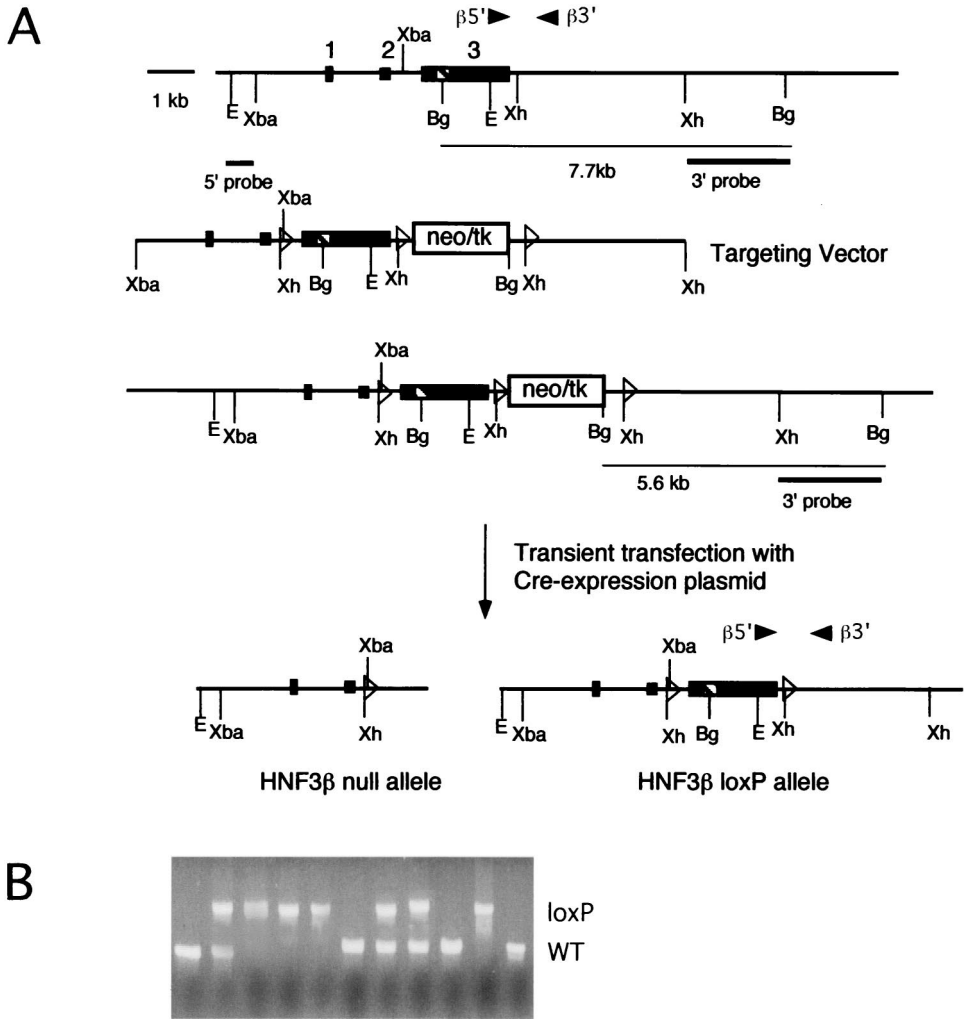

FIG. 1. Cre-loxP-mediated targeting of the *HNF3*β gene and generation of homozygous HNF3β$^{loxP/loxP}$ mice. (A) Targeting vector for the *HNF3*β^{loxP} allele. Primers β5′ and β3′ were used in PCR genotype analysis. (First line) Gene structure of the endogenous *HNF3*β locus. Exons are indicated as boxes, the striped box represents the winged helix domain, open triangles represent loxP sites, and arrow heads represent primer positions. (Second line) Targeting vector which introduces a cassette containing the neomycin-herpes simplex virus-thymidine kinase selection cassette (neo-tk) flanked by loxP sites downstream of exon 3. An additional loxP site was introduced in the intron upstream of exon 3. (Third line) Gene structure of homologous recombinants. The 3′ probe was used for the Southern blot analysis (data not shown). (Fourth line) Cre-mediated deletion results in either the *HNF3*β null allele (deletion of exon 3) or the *HNF3*β^{loxP} allele (exon 3 flanked by loxP sites). Abbreviations: Bg, *Bgl*II; E, *Eco*RI; Xh, *Xho*I; Xba, *Xba*I. (B) HNF3β$^{loxP/loxP}$ mice are viable and healthy. Shown are the results of PCR genotype analysis of a litter from mating HNF3β$^{loxP/+}$ heterozygotes inter se. The *HNF3*β^{loxP} allele segregates in expected Mendelian frequency. WT, wild type.

expression profile and metabolic regulation in these hepatocyte-specific HNF3β knockout mice.

MATERIALS AND METHODS

Generation of HNF3β$^{loxP/loxP}$ Alb.Cre mice. Lambda phage clones containing the murine HNF3β gene had been isolated from a mouse ES cell (strain 129) library previously (2). The targeting vector is depicted in Fig. 1A and contains approximately 5 kb of homology regions. This targeting construct was electroporated into E14/1 mouse ES cells (18). Stably transfected cells were isolated after selection in G418 (350 μg/ml; Gibco), and 340 clones were screened for the desired homologous recombination event. A 0.8-kb *Xho*I/*Bgl*II fragment (3′ probe in Fig. 1A) was used as an external probe for Southern blot analysis of DNA digested with *Bgl*II (data not shown). The *neo-tk* cassette was then removed from correctly targeted clones by partial Cre-mediated recombination. Two clones were expanded and transfected transiently with 2 μg of Cre expression vector (pIC-Cre [13]). Two days posttransfection, cells were treated with 2 μM gancyclovir to select for the cells that had lost the *neo-tk* cassette. Ninety-six individual gancyclovir-resistant clones were analyzed by Southern blotting (data not shown). Approximately 20% of the clones were identified to have undergone partial recombination to generate the HNF3β^{loxP} allele, thereby removing the *neo-tk* cassette and one loxP site but leaving both exon 3 and its flanking loxP sites intact. Two of the HNF3β^{loxP} ES cell clones were injected into C57BL/6J mouse blastocysts. Blastocysts were transferred to pseudopregnant NMRI females, and chimeric offspring were identified by the presence of agouti hair. Chimeric males were mated to C57BL/6 females to obtain ES cell-derived offspring that were analyzed by Southern blotting of tail DNA to identify the HNF3β$^{loxP/+}$ heterozygote mice. Germ line chimeras were crossed to CD1 outbred mice, as this is the strain of mice used previously for the analysis of the *HNF3*β null allele (2). Heterozygotes were mated inter se to generate homozygous HNF3β$^{loxP/loxP}$ mice. The derivation of the Alb.Cre transgenic line has been described previously (25), and mice were kept on a CD1 background.

Genotype analysis. The genotypes of all offspring were analyzed using DNA isolated either from the yolk sac of embryos or the tails of 4-week-old mice. The 5′ and 3′ primers for the *Alb.Cre* transgene (PCR product of 232 bp) were 5′-GCGGCATGGTGCAAGTTGAAT-3′ and 5′-CGTTCACCGGCATCAAC GTTT-3′, respectively. The 5′ and 3′ primers for the *HNF3*β gene whose positions are depicted in Fig. 1a were 5′-CCCCTGAGTTGGCGGTGGT-3′ and 5′-TTGCTCACGGAAGAGTAGCC-3′, respectively, which produce an ~290-bp amplified fragment for the wild-type *HNF3*β allele and an ~450-bp amplified fragment for the *HNF3*β^{loxP} allele. PCRs were carried out for 32 cycles (95°C for 45 s, 60°C for 45 s; 72°C for 90 s) in a buffer containing 1.5 mM $MgCl_2$.

Immunohistochemistry. Adult and fetal tissue samples were fixed in 4% paraformaldehyde overnight at 4°C, embedded in paraffin, cut to 6-μm-thick sections

and applied to Probe-on Plus slides (Fisher Scientific). Deparaffinized and rehydrated slides were subjected to microwave antigen retrieval by boiling for 6 min in a 10 mM citric acid buffer, pH 6.0, and allowed to cool for 10 min at room temperature (RT). Slides were washed in phosphate-buffered saline (PBS), then blocked with avidin and biotin blocking agent (Vector) for 15 min each at RT, and then blocked with protein blocking reagent (Immunotech) for 20 min at RT. The primary antibody, a 1:10,000 dilution of polyclonal rabbit anti-HNF-3β, kindly provided by Thomas M. Jessell (Columbia University, New York, N.Y.), was diluted in PBS containing 0.1% bovine serum albumin (BSA) and 0.2% Triton X-100 (PBT) and incubated with the sections overnight at 4°C. Slides were washed in PBS, then incubated with goat anti-rabbit biotinylated secondary antibody (Biomeda Biostain Rabbit IgG [AP] kit) diluted in PBT for 30 min at 37°C, washed in PBS, and incubated with alkaline phosphatase-conjugated ABC reagent (Biomeda) diluted in PBT for 30 min at 37°C. Slides were washed in PBS and then washed in a solution containing 100 mM NaCl, 50 mM $MgCl_2$, 100 mM Tris (pH 9.5), and 0.1% Tween 20. Signal was developed in Nitro Blue Tetrazolium (0.35 mg/ml; Boehringer Mannheim), BCIP (5-bromo-4-chloro-3-indolylphosphate (0.18 mg/ml; Boehringer Mannheim) for 8 min at RT. Slides were washed in water, counterstained in a 2% neutral red solution for 20 min, dehydrated, mounted, and viewed using Nomarski optics on a Nikon X4Z microscope.

RNA analysis and liver function tests. Northern blot, RNase protection, and reverse transcription-PCR analysis were performed as described previously (12, 16). The primers used for reverse-transcription-PCR are available upon request. Microarray hybridizations were carried out by Incyte Pharmaceuticals, Inc. (Palo Alto, Calif.). For liver function tests, mice were fasted for 9 h before sacrifice by carbon dioxide asphyxiation. Whole venous blood obtained from the inferior vena cava was mixed with an anticoagulant consisting of trasylol, EDTA, and leupeptin and centrifuged for 5 min at 14,000 × *g* to obtain plasma. Plasma parameters were determined by Ani Lytics, Inc. (Gaithersburg, Md.).

Preparation of nuclear extracts from liver. Livers from 16-week-old adult mice were extracted, rinsed in cold PBS, minced, and dounced in homogenization buffer (2 M sucrose, 10 mM HEPES (pH 7.6), 25 mM KCl, 1 mM EDTA, 0.15 mM spermine, 0.5 mM spermidine, 0.5 mM phenylmethylsulfonyl fluoride [PMSF], 0.5 mM dithiothreitol [DTT], and 10% glycerol) until most of the cells were disrupted but nuclei were still intact. The liver homogenates were then layered on top of homogenization buffer in an ultracentrifuge tube and centrifuged at 27,000 rpm (90,000 × *g*) for 55 min at 4°C. The nuclear pellet was resuspended in 0.1 ml of nuclear storage buffer (20 mM Tris [pH 7.9], 75 mM NaCl, 0.5 mM EDTA, 0.125 mM PMSF, 0.85 mM DTT, and 50% glycerol). A 0.01-ml aliquot of the nuclear pellet was used to normalize nuclear extract concentration as follows: 0.2 ml of 1% sodium dodecyl sulfate was added to the nuclear pellet aliquot, vortexed, and centrifuged at 15,000 × *g* for 3 min. Absorbance at 260 nm was assayed to estimate the amount of nucleic acid in the nuclear extract. The remainder of the nuclear extract was centrifuged at 3,000 rpm for 15 min at 4°C. The nuclei were resuspended in nuclear storage buffer at 25 μg/ml. Nine volumes of 1.1× NUN solution (27.5 mM HEPES [pH 7.6], 1.1 M urea, 0.33 M NaCl, 1.1 mM DTT, and 1.1% NP-40) was added, vortexed briefly, incubated on ice for 15 min, and centrifuged at 14,000 rpm at 4°C. Glycerol was added to the supernatant containing the nuclear extract to a 10% final volume and the solution was dialyzed against a 1,000× volume of Gorski dialysis buffer (25 mM HEPES [pH 7.9], 40 mM KCl, 0.1 mM EDTA, 0.5 mM PMSF, 1 mM DTT, and 10% glycerol) for 2 h at 4°C. Samples were subsequently centrifuged at 14,000 rpm for 1 min at 4°C, aliquoted, and stored at −80°C. Additionally, all buffers contained the following protease inhibitors: 0.1 mM benzamidine; 1 μg of antipain, leupeptin, and soybean trypsin inhibitor per ml; and 2 μg of aprotinin and bestatin per ml.

Electrophoretic mobility shift assays (EMSAs). The binding reaction contained 2.0 μg of nuclear extract in a 15-μl solution of 10 mM Tris (pH 7.5), 50 mM NaCl, 1 mM EDTA, 1 mM 2-mercaptoethanol, and 1% Ficoll, with 200 ng of poly(dI-dC) and 2 μg of bovine serum albumin. The mixtures were incubated at RT for 10 min, and then an 80-fold molar excess of competitor oligonucleotide (as indicated) and 0.1 ng (5×10^4 to 10×10^4 cpm) of oligonucleotide probe were added to the reaction mixture. Incubation was continued for an additional 20 min prior to electrophoresis on 8% polyacrylamide gels in 1× Tris-borate-EDTA, and gels were dried and exposed to a PhosphorImager cassette. Oligonucleotide probes were labeled with [^{32}P]dCTP by filling in the ends with Klenow polymerase I. The sequences of the double-stranded oligonucleotides used as probes or competitors have been described previously (9).

Glucose tolerance test. Overnight-fasted 8- to 15-week-old mice were injected intraperitoneally with 5 mg of glucose per g of body weight. Blood samples were obtained from the tail vein, and glucose levels were measured immediately before and 30, 60, and 120 min after injection using a Glucometer Elite device (Bayer, Inc.).

RESULTS

Generation of *HNF3*β^{loxP} mice. We have employed conditional gene inactivation using Cre-loxP-mediated recombination to study the role of HNF3β in the liver, as embryos homozygous for a *HNF3*β null allele die before hepatic differentiation begins (13, 25, 31). To achieve this, we constructed a targeting vector that introduced two loxP sites flanking exon 3 of the *HNF3*β gene, which contains the bulk of the protein-coding sequence, including the DNA binding domain (14), and a third loxP site downstream of a selection cassette consisting of the neomycin resistance and herpes simplex virus thymidine kinase genes (*neo-tk*) (Fig. 1A). We chose exon 3 because deletion of this exon in the germ line resulted in complete inactivation of the *HNF3*β gene (2, 33). After electroporation of mouse ES cells, screening of 340 neomycin (G418)-resistant colonies yielded three correctly targeted clones (data not shown). As the presence of the *neo-tk* cassette might interfere with the promoter activity and/or mRNA processing of the *HNF3*β gene, this *neo-tk* cassette was subsequently deleted in two of the targeted clones by transient transfection with a Cre expression vector. As depicted in Fig. 1A, this can result in either an *HNF3*β^{null} allele or the desired *HNF3*β^{loxP} allele. Southern blot analysis revealed approximately 20% of the 96 gangcyclovir-resistant clones tested to be HNF3β^{loxP} ES cell clones (data not shown). Germ line chimeras and mice heterozygous for the *HNF3*β^{loxP} allele were obtained for two independent ES cell lines injected. Both lines gave identical results in the tissue-specific gene ablation experiments.

To assess whether introduction of the two *loxP* sites in the second intron and 3′ untranslated region of the *HNF3*β gene affects gene function, heterozygous *HNF3*β^{loxP} mice were bred inter se, and the resulting offspring were genotyped by PCR analysis. Of 27 offspring genotyped at 4 weeks of age, seven were *HNF3*β$^{loxP/loxP}$, in close agreement with the expected Mendelian frequency (Fig. 1b). *HNF3*β$^{loxP/loxP}$ mice are fertile, healthy, and have normal growth curves (data not shown). Thus, insertion of the two *loxP* sites into the *HNF3*β locus does not appear to interfere with HNF3β function in this genetic background.

Ablation of the *HNF3*β gene in the liver. In order to investigate liver development and function in hepatocyte-specific HNF3β knockout mice, we utilized a transgenic mouse with Cre under the control of the albumin promoter (23). HNF3β^{loxP} heterozygous mice carrying this Alb.Cre transgene (HNF3β$^{loxP/+}$; Alb.Cre) were bred with HNF3β^{loxP} homozygous mice, and embryos were collected from various stages of gestation. As shown in Fig. 2A through F, no morphological abnormalities were observed in the livers of HNF3β$^{loxP/loxP}$; Alb.Cre embryos compared to their wild-type control littermates. Furthermore, adult livers that lack HNF3β have a normal morphology (compare Fig. 2G and H; also data not shown). HNF3β$^{loxP/loxP}$; Alb.Cre mice were born in the expected Mendelian distribution, and no significant differences in body weights were observed between these mice and their wild-type control littermates (data not shown). Liver-specific HNF3β knockout mice were fertile and produced normal-sized litters.

In light of the normal development of hepatic HNF3β knockout mice, we investigated whether we had indeed deleted the *HNF3*β gene in the liver. Therefore, steady-state HNF3β mRNA levels were analyzed in total liver RNA obtained from adult HNF3β$^{loxP/loxP}$; Alb.Cre or control mice using quantitative RNase protection analysis. HNF3β message was undetectable in the livers of 10-week-old HNF3β$^{loxP/loxP}$; Alb.Cre mice (Fig. 3A), indicating that the Cre recombinase had efficiently excised the loxP-flanked *HNF3*β gene in hepatocytes.

Next, we wanted to determine the stage of fetal development at which excision occurs. We analyzed the disappearance of HNF3β protein in livers obtained from HNF3β$^{loxP/loxP}$; Alb.Cre mice and their control littermates during various developmental stages using immunohistochemical staining with

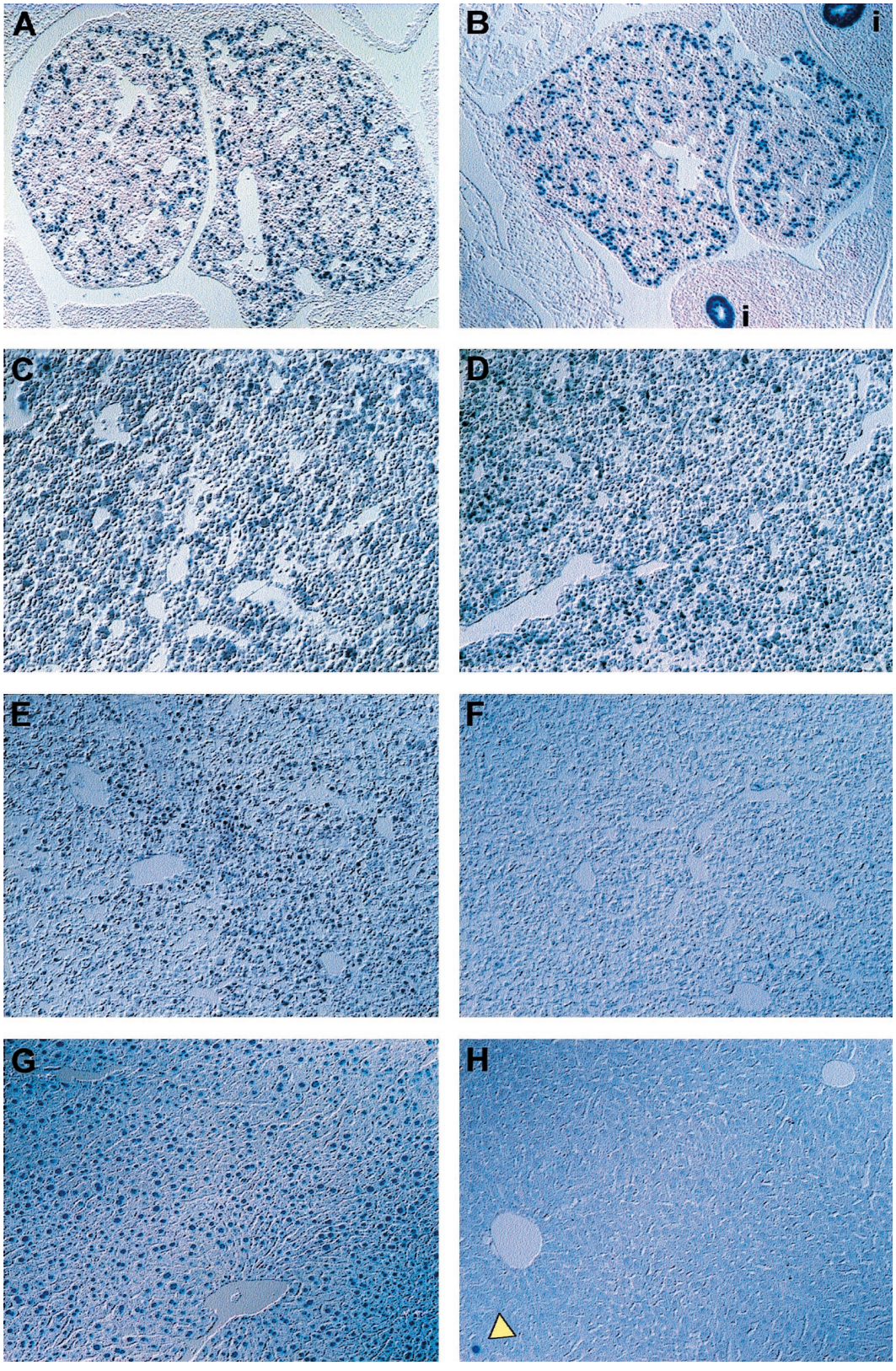

FIG. 2. The *HNF3β*^{loxP} allele is excised by the Alb.Cre transgene. (A to G) Immunohistochemical analysis of liver sections from 11.5 (A and B), 14.5 (C and D), and 18.5 (E and F) d.p.c. embryos and 10-week-old adult (G and H) mice stained with anti-HNF3β antibody. HNF3β$^{loxP/loxP}$; Alb.Cre mice express HNF3β by 14.5 d.p.c. (B and D), but HNF-3β protein is reduced in 18.5-d.p.c. fetal livers and absent from adult livers (F and H). The arrowhead in panel H shows a rare HNF3β immunoreactive nucleus. Images were obtained using Nomarski optics of livers from wild-type control mice (A, C, E, and G) and mutant HNF3β$^{loxP/loxP}$; Alb.Cre mice (B, D, G, and H). Images are shown at ×90 (A, B, G, and H) or ×180 (D to F) magnification.

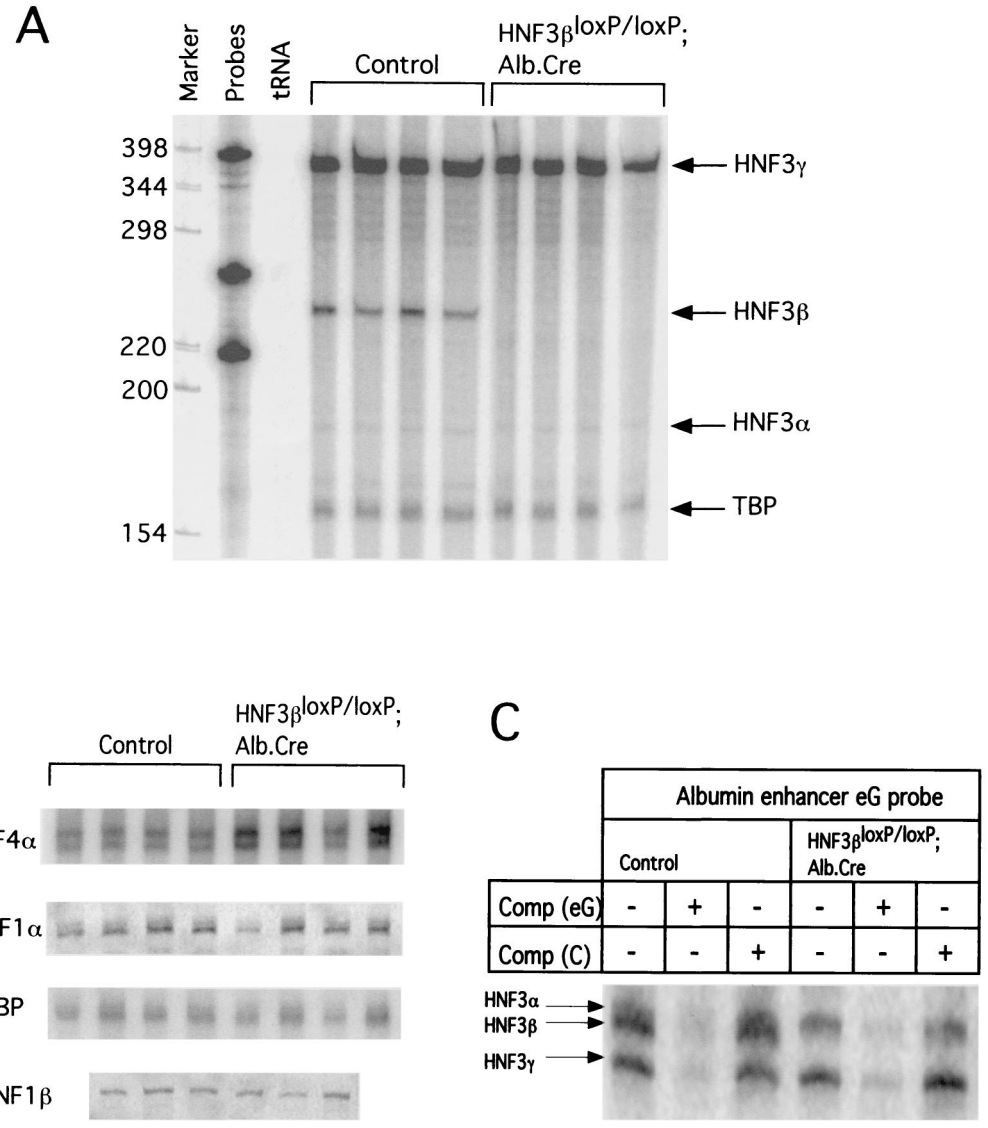

FIG. 3. Expression of hepatic transcription factors in adult livers from HNF3β$^{loxP/loxP}$; Alb.Cre. mice. (A) Total RNA (30 μg) from livers of wild type control or HNF3β$^{loxP/loxP}$; Alb.Cre mice was analyzed by RNase protection assay for mRNA levels of all *HNF3* genes. HNF3β mRNA is no longer expressed in livers of HNF3β$^{loxP/loxP}$; Alb.Cre mice, whereas HNF3α and HNF3γ steady-state mRNA levels are unchanged in HNF3β$^{loxP/loxP}$; Alb.Cre mice compared to controls. (B) Total RNA (30 μg) from livers of wild-type control or HNF3β$^{loxP/loxP}$; Alb.Cre mice was analyzed by RNase protection assay for mRNA levels of other liver-enriched *HNF* genes. HNF1α and HNF1β steady-state mRNA concentrations are unaltered whereas HNF4α mRNA levels are slightly increased in HNF3β$^{loxP/loxP}$; Alb.Cre mice compared to controls when quantitated using PhosphorImager analysis (data not shown). TATA box binding protein (TBP) served as the loading control. (C) Nuclear binding activities of HNF3α and HNF3γ are not increased in HNF3β$^{loxP/loxP}$; Alb.Cre hepatocytes compared to controls when analyzed using an EMSA. A radioactive oligonucleotide probe for the albumin enhancer eG site was incubated with 2 μg of nuclear extract isolated from wild-type control or HNF3β$^{loxP/loxP}$; Alb.Cre liver. An 80-fold molar excess of nonradioactive competitor oligonucleotide (Comp) was added as indicated: −, no indicated competitor added; eG, HNF3 binding site from albumin enhancer; C, non-specific competitor containing CCAAT site from albumin promoter. Specific HNF3 binding complexes are indicated. HNF3α and -β complexes from liver extracts migrate very closely together, as shown previously (9).

an antibody specific to HNF3β. Although the endogenous albumin promoter is active during the onset of liver development (approximately 9.5 days postcoitum [d.p.c.] in the mouse [4]), HNF3β inactivation was not evident in livers from midgestation HNF3β$^{loxP/loxP}$; Alb.Cre embryos (compare Fig. 2A and B and Fig. 2C and D). By 18.5 d.p.c., however, the vast majority of hepatocytes from such embryos had lost expression of HNF3β (compare Fig. 2E and F). HNF3β deletion is restricted to the liver, as HNF3β is still expressed in other organ systems where HNF3β is normally expressed (data not shown). Finally, HNF3β protein is missing in over 99.9% of hepatocytes in 10-week-old mice (compare Fig. 2G and H), consistent with the absence of HNF3β mRNA shown in Fig. 3A. Thus, we conclude that HNF3β is not required for the maintenance of hepatocytes in late fetal and postnatal development.

Ablation of *HNF3β* does not lead to dramatic changes in the hepatic transcriptional program. The expression of many genes required for yolk sac and liver metabolism, including apolipoproteins, aldolase B, and albumin, was dramatically decreased or completely absent in embryoid bodies derived from ES cells lacking HNF3β (12). In addition, expression of HNF3α was absent and that of HNF1α and HNF4α was reduced dramatically. As visceral endoderm differentiated in vitro expresses many of the same genes as hepatocytes in vivo,

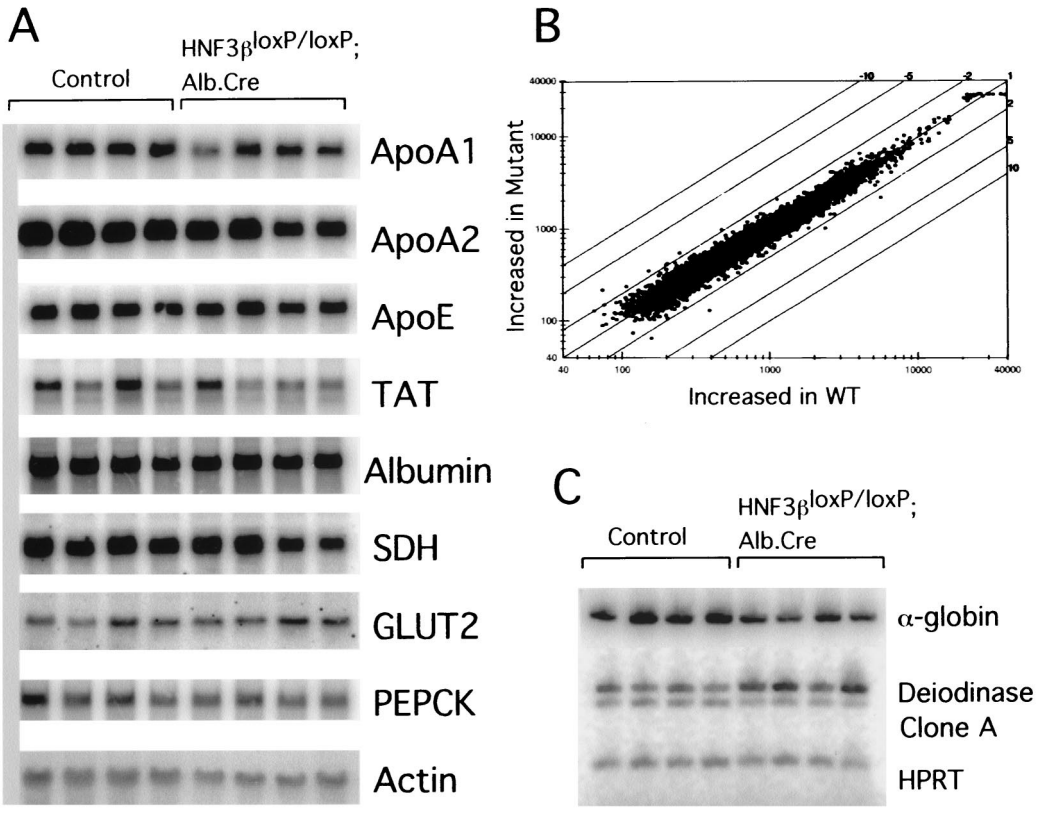

FIG. 4. Analysis of steady-state mRNA levels and microarray expression profile of potential HNF3 targets in liver. (A) Total RNA (10 μg) from livers of wild-type control (Control) or HNF3β$^{loxP/loxP}$; Alb.Cre mice was separated on denaturing agarose gels, blotted onto nylon membrane, and hybridized to the probes indicated (Apo, apolipoprotein; SDH, serine dehydrogenase; PEPCK, phosphoenolpyruvate carboxykinase; TAT, tyrosine amino transferase; GLUT2, glucose transporter 2). β-Actin (Actin) served as a loading control. PhosphorImager analysis did not reveal significant differences between the mRNA levels between the control and HNF3β$^{loxP/loxP}$; Alb.Cre mice (data not shown). (B) Scatter plot analysis representing expression profiles between livers from wild-type control and HNF3β$^{loxP/loxP}$; Alb.Cre mice using an oligonucleotide microarray representing 8,700 mouse cDNA and EST transcripts. (C) Reverse transcription-PCR analysis of total RNA from livers of wild-type control (Control) or HNF3β$^{loxP/loxP}$; Alb.Cre mice using [α-^{32}P]dATP. Steady-state mRNA levels of α-globin (accession no. AA109900) is decreased twofold, whereas deiodinase (accession no. AA212899) is induced twofold in livers of HNF3β$^{loxP/loxP}$; Alb.Cre mice compared to controls. Signals were quantified using PhosphorImager analysis (data not shown). Clone A (accession no. AA267590) EST mRNA levels were not significantly different between wild-type and mutant livers, although the microarray hybridization had indicated a threefold difference.

the notion was put forward that HNF3β directs a regulatory network of transcription factors and their targets in the metabolism of yolk sac and liver. However, as shown in Fig. 4A expression levels of mRNAs encoding apolipoproteins, albumin, and gluconeogenic enzymes are not significantly reduced in adult livers of HNF3β^{loxP}; Alb.Cre mice, despite the fact that these livers are devoid of HNF3β mRNA and protein.

In several knockouts of transcription factors belonging to gene families, targeted mutation of one gene led to an upregulation of other family members, demonstrating the existence of regulatory networks between these transcription factors (15, 26). As mentioned above, HNF3β also regulates a network of transcription factors in visceral endoderm differentiated from embryoid bodies in vitro that includes HNF1α, HNF4α, and HNF3α (12). Therefore, we analyzed the steady-state mRNA levels of these genes by quantitative RNase protection assay. Consistent with the findings by Duncan et al. (12), mRNA levels of HNF3γ were unchanged in the livers from mutant animals (Fig. 3A). However, in contrast to the situation in embryoid bodies, there was no decrease in the transcript levels of HNF3α or HNF1α but a small (60%) increase in HNF4α relative mRNA levels in liver (Fig. 3A and B). Furthermore, the relative mRNA levels for HNF1β and other liver-enriched transcription factors are unaffected (Fig. 3B and data not shown).

To address the possibility that the remaining HNF3 factors could compensate for lack of HNF3β function at a posttranscriptional level via increased protein stabilization or nuclear localization, we assayed nuclear HNF3 binding activity of hepatocytes that lack HNF3β and compared these to wild-type controls using an electrophoretic mobility shift assay with the albumin enhancer eG site, which contains an HNF3 binding site, as a probe. As demonstrated in Fig. 3C, there is no upregulation of HNF3α or HNF3γ nuclear binding activity in hepatocyte nuclei that lack HNF3β protein.

To identify other potential liver-specific targets of HNF3β, we used mRNA from livers of 10-week-old HNF3β$^{loxP/loxP}$; Alb.Cre mice and wild-type control littermates and screened for altered expression profiles using cDNA and expressed sequence tag (EST) microarray hybridization. As shown in the scatter plot in Fig. 4B, the overall transcriptional program is strikingly similar in livers containing or lacking HNF3β. Out of 8,700 mouse transcripts analyzed, three genes were reduced approximately two- to threefold in livers that lack HNF3β compared to control livers (Fig. 4B), whereas one gene was induced by more than twofold. To confirm whether differences

TABLE 1. Circulating intermediates in plasma in HNF3β$^{loxP/loxP}$; Alb.Cre and control mice[a]

Intermediate	Concn in plasma in mice		Reference range (concn)
	Control	HNF3β$^{loxP/loxP}$; Alb.Cre	
Creatine phosphokinase (U/liter)	2,241 ± 1,445	2,114 ± 574	0 – 800
Lactate dehydrogenase (U/liter)	581 ± 120	580 ± 86	260 – 680
AST-SGOT[b] (U/liter)	150 ± 36	139 ± 21	72 – 288
ALT-SGPT[c] (U/liter)	60 ± 29	32 ± 4	24 – 140
Gamma glutamyl transferase (U/liter)	0 ± 0	0.83 ± 0.50	0 – 2
Amylase (U/liter)	2,199 ± 160	2,778 ± 303	602 – 2,311
Bilirubin, total (mg/dl)	0.67 ± 0.45	0.27 ± 0.05	0.0 – 0.9
Bilirubin, direct (mg/dl)	0.13 ± 0.09	0.07 ± 0.03	0.0 – 0.2
Uric acid (mg/dl)	4.4 ± 1.9	1.9 ± 0.2	2.2 – 4.6
Blood urea nitrogen (mg/dl)	21.3 ± 1.4	19.8 ± 1.5	9.0 – 28.0
Creatinine (mg/dl)	0.38 ± 0.03	0.33 ± 0.03	0.2 – 0.7
Albumin (g/dl)	2.9 ± 0.5	2.3 ± 0.4	2.6 – 4.6
Protein, total (g/dl)	4.7 ± 0.2	3.9 ± 0.4	4.0 – 6.2

[a] Metabolic parameters were experimentally determined or analyzed by Ani Lytics, Inc., as described under Materials and Methods. Values are represented as means ± standard errors of the means. Comparisons were made among mice of similar age and sex (n = 6 animals for each group).
[b] Aspartate aminotransferase-serum glutamic oxalacetic transaminase.
[c] Alanine aminotransferase-serum glutamic pyruvic transaminase.

revealed by the microarray hybridization were real and not just an artifact of the assay, the transcript abundance of three of these differentially expressed genes was analyzed by quantitative reverse transcription-PCR in livers of HNF3β$^{loxP/loxP}$; Alb.Cre mice and control mice (Fig. 4C). After first determining the number of PCR cycles required for exponential amplification for each primer pair (data not shown), we compared mRNA levels in livers from four wild-type control and four mutant animals. As shown in Fig. 4C, deiodinase mRNA levels are induced two-fold in livers that lack HNF3β, in close agreement with the result from the array hybridization. Likewise, α-globin mRNA levels were reduced by approximately two-fold, as had been indicated by the microarray data. These results confirm the usefulness of microarray hybridization for obtaining accurate comparisons of the global transcriptional program between wild-type and mutant animals. These very limited changes in the overall gene expression pattern between HNF3β wild-type and mutant livers also argue that HNF3β is not required for the maintenance of the global hepatic transcriptional program.

Physiological consequence of hepatocyte-specific *HNF3*β gene inactivation. To assess whether loss of HNF3β in the liver affects liver metabolism of the HNF3β^{loxP}; Alb.Cre mice, we measured various serum parameters that are indicative of hepatic metabolism. There were no significant differences in these parameters between HNF3β^{loxP}; Alb.Cre mice and wild-type control littermates, as summarized in Table 1.

Many liver-specific genes that encode glycolytic or gluconeogenic enzymes have an HNF3 binding site located in their *cis*-regulatory element. Embryoid bodies derived from ES cells lacking HNF3β have decreased or absent expression of the genes encoding the glycolytic enzymes L-type pyruvate kinase and aldolase B (12). As HNF3β potentially regulates genes required for normal glucose homeostasis in vivo, we performed glucose tolerance tests on adult HNF3β^{loxP}; Alb.Cre mice and wild-type control littermates to examine whether they respond normally to a glucose challenge. Mice that lack hepatic HNF3β clear excess blood glucose at a rate similar to that of their wild-type control littermates (Fig. 5). Therefore, hepatic HNF3β appears not essential for normal glucose homeostasis in vivo.

DISCUSSION

We have employed conditional gene ablation of *HNF3*β using the Cre-loxP recombination system to generate a mouse model that lacks *HNF3*β specifically in the liver. While hepatocyte-specific inactivation of *HNF3*β was greater than 99.9% efficient in the adult liver, inactivation of *HNF3*β gene expression was not evident until the end of fetal development, although the albumin gene is activated on day 9 of gestation (4). A similar temporal discrepancy between Cre expression and gene inactivation has been observed when the *Pdx1* gene was ablated in β-cells of the pancreas using the Cre-loxP system (1). Several factors could account for this delay in gene inactivation. First, plasmid transgene expression levels depend on the choice of the promoter as well as position effects after insertion of the transgene into the genome. Secondly, before HNF3β (or PDX1) protein expression is extinguished, Cre must first be expressed by the tissue-specific promoter and

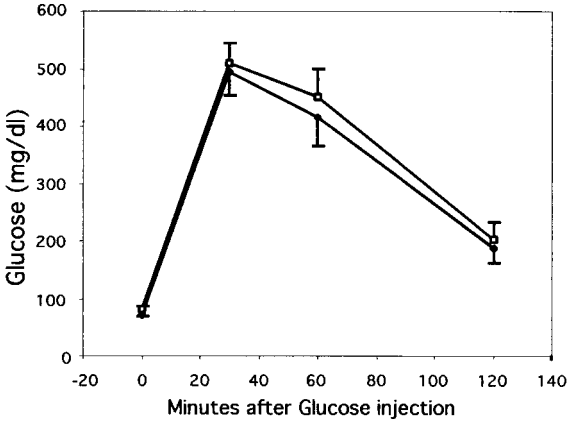

FIG. 5. Mice lacking hepatic HNF3β have normal glucose homeostasis. Glucose challenge of age-matched HNF3β$^{loxP/loxP}$; Alb.Cre (□) and wild-type control (◆) mice. Blood glucose levels are shown at indicated time points after intraperitoneal administration of glucose. Values are means ± standard errors of the means (error bars) of seven (control) or nine (HNF3β$^{loxP/loxP}$; Alb.Cre) animals. There was no significant difference between experimental and control groups as determined by Students's t test for each time point.

transported to the nucleus where it must recombine both *loxP*-flanked alleles. Finally, depending on the half-life of the mRNA and protein remaining after Cre-mediated recombination, hours or days might be required until expression is completely lost. Therefore, using the HNF3β$^{loxP/loxP}$; Alb.Cre mice we were unable to determine whether *HNF3*β has a role in initiating the hepatic differentiation program during early liver development, as *HNF3*β was still present at this time. A Cre transgene expressed specifically in the prehepatic endoderm may be used in the future to investigate whether *HNF3*β is required for organogenesis of the liver from foregut endoderm.

Analyses of the promoters of liver-specific genes have identified binding sites for multiple transcription factors, leading to the hypothesis that cooperation between several liver-enriched transcription factors regulates hepatic gene expression (reviewed in reference 5). This model would predict that loss of one transcription factor alone would have minor consequences for the global liver gene expression profile. In contrast to this model, the idea has been put forth that a transcriptional hierarchy among the liver-enriched transcription factors exists to maintain the hepatic transcriptional program (11, 12, 19, 30). Visceral endoderm expresses many genes encoding metabolic enzymes also active in the liver. For this reason, the contribution of HNF3β to their regulation was investigated in visceral endoderm derived from embryoid bodies lacking *HNF3*β (12). Under these in vitro conditions, loss of *HNF3*β resulted in a dramatic alteration in mRNA abundance of the genes encoding hepatocyte-enriched transcription factors (HNF3α, HNF1α, and HNF4α) and their target genes that are involved in normal hepatic metabolism and differentiation. In contrast, mice lacking *HNF3*β in the liver exhibited only minor changes in the transcriptional program.

Several explanations could account for the mild hepatic phenotype in HNF3β$^{loxP/loxP}$; Alb.Cre mice. First, compensatory binding by HNF3α and HNF3γ proteins could explain the largely unchanged hepatic gene expression profile. It has been shown, for instance, that HNF3α can bind to and transactivate the same *cis*-regulatory elements as HNF3β in a native chromosomal context (12). However, our evidence clearly shows the lack of upregulation of the remaining *HNF3* genes at either the transcriptional (Fig. 3A) or posttranscriptional level (Fig. 3C) in livers from HNF3β$^{loxP/loxP}$; Alb.Cre mice, in contrast to what had been observed in livers from *HNF3*γ mutant animals (15). Alternatively, hepatic gene expression may be redundantly regulated by a combination of liver-enriched and ubiquitous transcription factors, any one of which might play only a minor role in its regulation. This notion is supported by gene targeting of HNF1α, in which many of the previously known HNF1α targets identified in vitro were not altered in the mutant animals (24).

In summary, *HNF3*β gene targeting studies have identified several steps in mammalian development that are critically dependent on *HNF3*β. Regarding endoderm development, these include the formation of a functional node, from which definite endoderm is derived, the development of foregut and midgut (but not hindgut) endoderm, and the differentiation of functionally competent visceral endoderm (2, 10, 33). While the molecular targets of HNF3β in the development of the node and definitive endoderm are largely unknown, it appears that the activation of HNF4α and HNF1α and their target genes are dependent on HNF3β in visceral endoderm, at least in vitro. However, our studies have shown that gene regulation in visceral endoderm and liver are not necessarily parallel, as HNF3β is not required for the maintenance of the network of HNF transcription factors or for the global transcriptional program in hepatocytes.

ACKNOWLEDGMENTS

N.J.S. and S.-L.A. contributed equally to this work.

We are grateful to M. Birnbaum, L. Greenbaum, and M. A. Lazar for critical reading of the manuscript; T. Jessell for providing the HNF3β antibody; K. Zaret, P. Bossard, and L. Greenbaum for providing assistance with the preparation of nuclear extracts and the EMSA; R. Ahima for assistance with the glucose tolerance test; and G. Schütz for his support during the initial phase of the project.

Our studies were facilitated by the Center for Molecular Studies in Digestive and Liver Disease at the University of Pennsylvania (P30 DK50306). This work was supported by the NIDDK (RO1 DK55342 to KHK and RO1s DK42502 and DK42612 to MAM), the Association pour la Recherche sur le Cancer, the Institut National de la Santé et de la Recherche Médicale, the Centre National de la Recherche Scientifique, and the Centre Hospitalier Universitaire Régional (grant to S.L.A.). N.J.S. was supported through an NIH pre-doctoral training grant (5-T32-GM08216).

REFERENCES

1. **Ahlgren,U., J. Jonsson, L. Jonsson, K. Simu, and H. Edlund.** 1998. beta-cell-specific inactivation of the mouse Ipf1/Pdx1 gene results in loss of the beta-cell phenotype and maturity onset diabetes. Genes Dev. **12:**1763–1768.
2. **Ang, S. L., and J. Rossant.** 1994. HNF-3 beta is essential for node and notochord formation in mouse development. Cell **78:**561–574.
3. **Ang, S. L., A. Wierda, D. Wong, K. A. Stevens, S. Cascio, J. Rossant, and K. S. Zaret.** 1993. The formation and maintenance of the definitive endoderm lineage in the mouse: involvement of HNF3/forkhead proteins. Development **119:**1301–1315.
4. **Cascio, S., and K. S. Zaret.** 1991. Hepatocyte differentiation initiates during endodermal-mesenchymal interactions prior to liver formation. Development **113:**217–225.
5. **Cereghini, S.** 1996. Liver-enriched transcription factors and hepatocyte differentiation. FASEB J. **10:**267–282.
6. **Cirillo, L. A., C. E. McPherson, P. Bossard, K. Stevens, S. Cherian, E. Y. Shim, K. L. Clark, S. K. Burley, and K. S. Zaret.** 1998. Binding of the winged-helix transcription factor HNF3 to a linker histone site on the nucleosome. EMBO J **17:**244–254.
7. **Clark, K. L., E. D. Halay, E. Lai, and S. K. Burley.** 1993. Co-crystal structure of the HNF-3/fork head DNA-recognition motif resembles histone H5. Nature **364:**412–420.
8. **Costa, R. H., D. R. Grayson, and J. J. Darnell.** 1989. Multiple hepatocyte-enriched nuclear factors function in the regulation of transthyretin and alpha 1-antitrypsin genes. Mol. Cell. Biol. **9:**1415–1425.
9. **DiPersio, C. M., D. A. Jackson, and K. S. Zaret.** 1991. The extracellular matrix coordinately modulates liver transcription factors and hepatocyte morphology. Mol. Cell. Biol. **11:**4405–4414.
10. **Dufort, D., L. Schwartz, K. Harpal, and J. Rossant.** 1998. The transcription factor HNF3beta is required in visceral endoderm for normal primitive streak morphogenesis. Development **125:**3015–3025.
11. **Duncan, S. A., A. Nagy, and W. Chan.** 1997. Murine gastrulation requires HNF-4 regulated gene expression in the visceral endoderm: tetraploid rescue of Hnf-4(−/−) embryos. Development **124:**279–287.
12. **Duncan, S. A., M. A. Navas, D. Dufort, J. Rossant, and M. Stoffel.** 1998. Regulation of a transcription factor network required for differentiation and metabolism. Science **281:**692–695.
13. **Gu, H., J. D. Marth, P. C. Orban, H. Mossmann, and K. Rajewsky.** 1994. Deletion of a DNA polymerase beta gene segment in T cells using cell type-specific gene targeting. Science **265:**103–106.
14. **Kaestner, K. H., H. Hiemisch, B. Luckow, and G. Schütz.** 1994. The HNF-3 gene family of transcription factors in mice: gene structure, cDNA sequence, and mRNA distribution. Genomics **20:**377–385.
15. **Kaestner, K. H., H. Hiemisch, and G. Schütz.** 1998. Targeted disruption of the gene encoding hepatocyte nuclear factor 3γ results in reduced transcription of hepatocyte-specific genes. Mol. Cell. Biol. **18:**4245–4251.
16. **Kaestner, K. H., J. Katz, Y. Liu, D. J. Drucker, and G. Schütz.** 1999. Inactivation of the winged helix transcription factor HNF3alpha affects glucose homeostasis and islet glucagon gene expression in vivo. Genes Dev. **13:**495–504.
17. **Kaestner, K. H., W. Knochel, and D. E. Martinez.** 2000. Unified nomenclature for the winged helix/forkhead transcription factors. Genes Dev. **14:**142–146.
18. **Kühn, R., K. Rajewski, and W. Müller.** 1991. Generation and analysis of interleukin-4 deficient mice. Science **254:**707–710.
19. **Kuo, C. J., P. B. Conley, L. Chen, F. M. Sladek, J. E. Darnell, Jr., and G. R. Crabtree.** 1992. A transcriptional hierarchy involved in mammalian cell-type specification. Nature **355:**457–461.

20. **Lai, E., V. R. Prezioso, E. Smith, O. Litvin, R. H. Costa, and J. E. Darnell, Jr.** 1990. HNF-3A, a hepatocyte-enriched transcription factor of novel structure is regulated transcriptionally. Genes Dev. **4:**1427–1436.
21. **Lai, E., V. R. Prezioso, W. F. Tao, W. S. Chen, and J. E. Darnell, Jr.** 1991. Hepatocyte nuclear factor 3 alpha belongs to a gene family in mammals that is homologous to the Drosophila homeotic gene fork head. Genes Dev. **5:**416–427.
22. **McPherson, C. E., E. Y. Shim, D. S. Friedman, and K. S. Zaret.** 1993. An active tissue-specific enhancer and bound transcription factors existing in a precisely positioned nucleosomal array. Cell **75:**387–398.
23. **Monaghan, A. P., K. H. Kaestner, E. Grau, and G. Schütz.** 1993. Postimplantation expression patterns indicate a role for the mouse forkhead/HNF-3 alpha, beta and gamma genes in determination of the definitive endoderm, chordamesoderm and neuroectoderm. Development **119:**567–578.
24. **Pontoglio, M., J. Barra, M. Hadchouel, A. Doyen, C. Kress, J. P. Bach, C. Babinet, and M. Yaniv.** 1996. Hepatocyte nuclear factor 1 inactivation results in hepatic dysfunction, phenylketonuria, and renal Fanconi syndrome. Cell **84:**575–585.
25. **Postic, C., M. Shiota, K. D. Niswender, T. L. Jetton, Y. Chen, J. M. Moates, K. D. Shelton, J. Lindner, A. D. Cherrington, and M. A. Magnuson.** 1999. Dual roles for glucokinase in glucose homeostasis as determined by liver and pancreatic beta cell-specific gene knock-outs using Cre recombinase. J. Biol. Chem. **274:**305–315.
26. **Rudnicki, M. A., T. Braun, S. Hinuma, and R. Jaenisch.** 1992. Inactivation of MyoD in mice leads to up-regulation of the myogenic HLH gene Myf-5 and results in apparently normal muscle development. Cell **71:**383–390.
27. **Sasaki, H., and B. L. Hogan.** 1993. Differential expression of multiple fork head related genes during gastrulation and axial pattern formation in the mouse embryo. Development **118:**47–59.
28. **Shih, D. Q., M. A. Navas, S. Kuwajima, S. A. Duncan, and M. Stoffel.** 1999. Impaired glucose homeostasis and neonatal mortality in hepatocyte nuclear factor 3alpha-deficient mice. Proc. Natl. Acad. Sci. USA **96:**10152–10157.
29. **Shim, E. Y., C. Woodcock, and K. S. Zaret.** 1998. Nucleosome positioning by the winged helix transcription factor HNF3. Genes Dev. **12:**5–10.
30. **Stoffel, M., and S. A. Duncan.** 1997. The maturity-onset diabetes of the young (MODY1) transcription factor HNF4alpha regulates expression of genes required for glucose transport and metabolism. Proc. Natl. Acad. Sci. USA **94:**13209–13214.
31. **Tsien, J. Z., D. F. Chen, D. Gerber, C. Tom, E. H. Mercer, D. J. Anderson, M. Mayford, E. R. Kandel, and S. Tonegawa.** 1996. Subregion- and cell type-restricted gene knockout in mouse brain. Cell **87:**1317–1326.
32. **Weigel, D., G. Jurgens, F. Kuttner, E. Seifert, and H. Jäckle.** 1989. The homeotic gene fork head encodes a nuclear protein and is expressed in the terminal regions of the Drosophila embryo. Cell **57:**645–658.
33. **Weinstein, D. C., A. Ruiz i Altaba, W. S. Chen, P. Hoodless, V. R. Prezioso, T. M. Jessell, and J. E. Darnell, Jr.** 1994. The winged-helix transcription factor HNF-3 beta is required for notochord development in the mouse embryo. Cell **78:**575–588.
34. **Zaret, K. S.** 1996. Molecular genetics of early liver development. Annu. Rev. Physiol. **58:**231–251.